

Electronic Charge Order in the Pseudogap State of $\text{Bi}_2\text{Sr}_2\text{CaCu}_2\text{O}_{8+\delta}$

Y. H. Liu, K. Takeyama, T. Kurosawa, N. Momono, M. Oda and M. Ido
Department of Physics, Hokkaido University, Sapporo 060-0810, Japan

Scanning tunneling microscopy/spectroscopy is used to examine the $4a \times 4a$ electronic charge order (CO) in the pseudogap (PG) state above T_c on $\text{Bi}_2\text{Sr}_2\text{CaCu}_2\text{O}_{8+\delta}$. It is demonstrated that the static CO develops markedly in the inhomogeneous PG state, while it is very weak in the homogeneous PG state. We suggest that this static CO, which is considered to be stabilized by the pinning of the dynamically fluctuating CO, will remain below T_c , together with the inhomogeneous gap structure, and coexist with the superconductivity.

PACS numbers: 68.37.Ef, 74.72.Hs, 74.25.-q, 74.50.+r

In high- T_c cuprate superconductors, it has been established that an unusual electronic state, characterized by a gap-like structure around the Fermi level E_F , the so-called “pseudogap (PG)”, develops in the normal state above T_c , and it must be well understood to elucidate the mechanism of high- T_c superconductivity. Recently, in the PG state of underdoped (UD) $\text{Bi}_2\text{Sr}_2\text{CaCu}_2\text{O}_{8+\delta}$ (Bi2212), Vershinin *et al.* [1] found a charge order (CO) in two-dimensional (2D) maps of the local density of states (LDOS) at specified energies, which were obtained by scanning tunneling microscopy/spectroscopy (STM/STS). This CO is oriented along the two Cu-O bond directions, intersecting at right angles; its period is independent of energy, $4.5a \sim 4.8a$ along each Cu-O direction (a : the lattice constant or the Cu-O-Cu distance), which is called “nondispersive.” Interestingly, the nondispersive CO develops markedly at low energies within the PG and tends to disappear outside the PG. On the other hand, in the SC state, they did not observe the nondispersive CO, but observed dispersive LDOS modulations due to quasiparticle interference effects, which were first reported by Hoffman *et al.* [2]. This tempted many researchers to suppose that the nondispersive CO is a characteristic feature only for the PG state above T_c .

However, in the SC state of UD Bi2212, Howald *et al.* [3] and Momono *et al.* [4] observed a nondispersive CO, whose period, $\sim 4a$ for each Cu-O direction, was smaller than that reported by Vershinin *et al.* in the PG state. Furthermore, it has recently been demonstrated in STM/STS experiments by Hashimoto *et al.* [5] that the amplitude of $4a \times 4a$ CO at $T \ll T_c$ is strongly sample-dependent; in samples exhibiting an intense $4a \times 4a$ CO at $T \ll T_c$, the spatial dependence of the energy gap structure is inhomogeneous on the nanometer scale, and vice versa. Whether the $4a \times 4a$ CO is a common feature for both the SC and PG states is of great interest for elucidating the relation among the CO, PG and high- T_c superconductivity. In this paper, we report STM/STS experiments in the PG state above T_c on two kinds of samples that exhibit strong and weak $4a \times 4a$ CO's at $T \ll T_c$, as shown in Figs. 2 (d) and (e), and suggest that the static $4a \times 4a$ CO, which develops markedly in the in-

homogeneous PG state, will remain below T_c , together with the inhomogeneous gap structure, and coexist with the superconductivity.

Bi2212 crystals were grown by the traveling solvent floating zone method. The T_c was determined to be 81 K from the SC diamagnetic transition curve, and the hole doping level p was estimated to be slightly UD, ~ 0.14 . The details of this estimation have been reported in Ref. 7. In this study, two samples, labeled L and M, were cleaved in a vacuum of $< 10^{-9}$ torr at liquid-nitrogen temperature and room temperature, respectively, before being inserted in situ into an STM unit at ~ 7 K. It should be noted that STM/STS experiments in the PG state were performed after finishing those at $T \ll T_c$ and warming the sample gradually in situ up to a temperature above T_c . STM images were taken in the constant-height mode; under the constant sample-bias voltage V_s , the tip-height, determined by giving the initial value I_t^0 for tunneling current I_t at the initial tip-position, was kept constant during the tip scanning, where I_t was measured as a function of tip-position.

As is well known, the cleavage in Bi2212 usually occurs between the semiconducting Bi-O planes with an energy gap E_g of the order of 100 meV, forming a bilayer, in which excess oxygen ions, providing the Cu-O plane nearby with mobile holes, are contained. In STM experiments on the cleaved surface, the top most atomic plane closest to the tip is the semiconducting Bi-O plane, the second the insulating Sr-O plane and the third the metallic or SC Cu-O plane, and we can observe the different planes selectively, as reported in Refs. 6 and 8; STM images measured at $V_s > E_g/e \sim 100$ mV reflect the Bi-O plane, while STM images measured at $V_s \lesssim 100$ mV mainly reflect the Cu-O plane. Here, we focus on low-bias STM images reflecting the Cu-O plane.

Shown in Fig. 1 (a) is an STM image measured at $V_s = 30$ mV on sample L in the PG state ($T = 85$ K) above T_c . One can see a 2D charge modulation or a 2D CO clearly. It is locally distorted but oriented along the Cu-O directions tilted by 45° from a weak 1D superstructure. The 1D superstructure is observed much more evidently at high voltages of several hundred mV ($> E_g/e$),

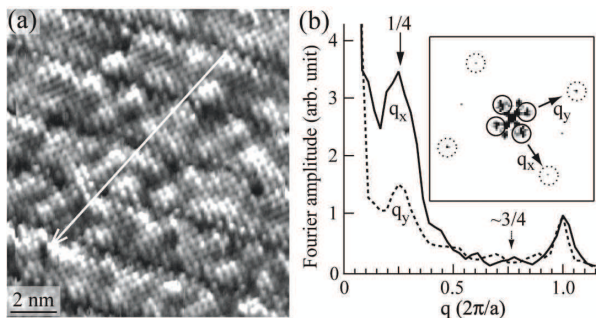


FIG. 1: (a) STM image for an area of sample L, obtained at $T = 85$ K, $V_s = 30$ mV and $I_t^0 = 0.18$ nA. (b) Line cuts taken along the q_x and q_y directions on the Fourier map (inset).

because it is a striking feature of the Bi-O plane [7]. To quantify the period of 2D CO, we performed a Fourier transform on the image. The Fourier map is shown in the inset of Fig. 1 (b), where four spots surrounded by dotted-line circles correspond to the atomic periodicity and four broad spots surrounded by solid-line circles near the origin result from the periodic CO. The most intense peaks appearing at $(2\pi/4a, 0)$ and $(0, 2\pi/4a)$ in the line cuts (Fig. 1 (b)) taken along the q_x and q_y directions on the Fourier map indicate that the 2D CO has an average period of $4a \times 4a$. Very small peaks at around $(6\pi/4a, 0)$ and $(0, 6\pi/4a)$ seem to correspond to the internal structure of the CO, which has been observed clearly in the low-temperature PG state of lightly-doped $\text{Ca}_{2-x}\text{Na}_x\text{CuO}_2\text{Cl}_2$ [8].

Figure 2 (a) shows an STM image measured at $V_s = 30$ mV in another area of sample L, ~ 60 nm from the former area where the STM image of Fig. 1 (a) was taken. A similar CO can be seen throughout this image. The Fourier analysis verified that the CO in Fig. 2 (a) had a period of $4.4a \times 4.4a$, which was slightly larger than that in Fig. 1 (a). STM measurements in several other areas, where a CO can be clearly seen in low-bias images with an atomic resolution, demonstrated that the period of the CO, distributed slightly in the range from $4a$ to $4.4a$, was smaller than the value ($4.5a \sim 4.8a$) reported by Vershinin *et al* in the PG state [1], but almost the same as in the SC state of sample L. Hereafter, we denote the period near four times the lattice-constant as $\sim 4a \times 4a$.

From the V_s -dependence of the STM image in the latter area of sample L, it was found that the period of the CO was energy-independent, *i.e.* nondispersive, while its amplitude decreased rapidly with increasing energy and became negligibly small above the PG energy, $\sim \Delta_{\text{PG}}$, as shown in the inset of Fig. 2 (c). This, consistent with the result observed by Vershinin *et al.* [1], indicates that the characteristic energy of the $\sim 4a \times 4a$ charge order in the PG state above T_c is the corresponding energy gap, as in the SC state below T_c [4, 5].

Figure 2 (b) shows an STM image in the PG state of

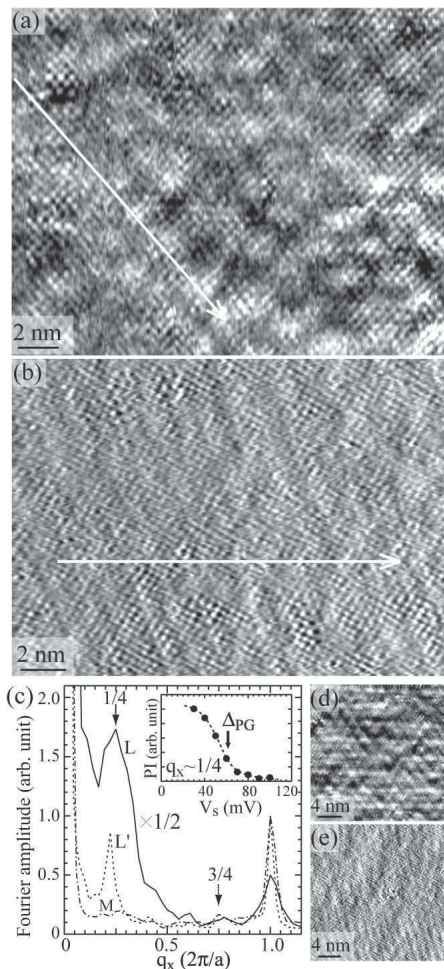


FIG. 2: (a) STM image for an another area (L') of sample L obtained at $T = 85$ K, $V_s = 30$ mV and $I_t^0 = 0.18$ nA. (b) STM image for sample M obtained at $T = 88$ K, $V_s = 20$ mV and $I_t^0 = 0.18$ nA. (c) Line cuts taken along the q_x direction on the Fourier maps corresponding to the two areas of sample L and sample M. Inset: V_s -dependence of the peak intensity (PI) at $q_x \sim 2\pi/4a$ measured in the latter area (L') of sample L. The PI reaches the background level above $V_s \sim 90$ mV. (d) and (e) STM images for samples L and M obtained at $T \sim 7$ K in the SC state, respectively ($V_s = 30$ mV).

sample M, measured at $T = 88$ K and $V_s = 20$ mV, which was the lowest of the examined bias voltages. For this sample, similar images were obtained at $V_s \lesssim 100$ mV. In the low-bias image of sample M, one can see that an atomic resolution is obtained as in those of sample L, while the CO is too weak to be distinguished; indeed, the peak at $(\sim 2\pi/4a, 0)$ in the Fourier map (Fig. 2 (c)), corresponding to the $\sim 4a \times 4a$ CO, is rather small compared with the Bragg peak at $(2\pi/a, 0)$. The former fact guarantees that the obtained image is reliable, and it is therefore concluded that such a weak CO is an intrinsic property in the PG state of sample M. Thus, the present two samples, L and M, exhibit strong and weak CO's in

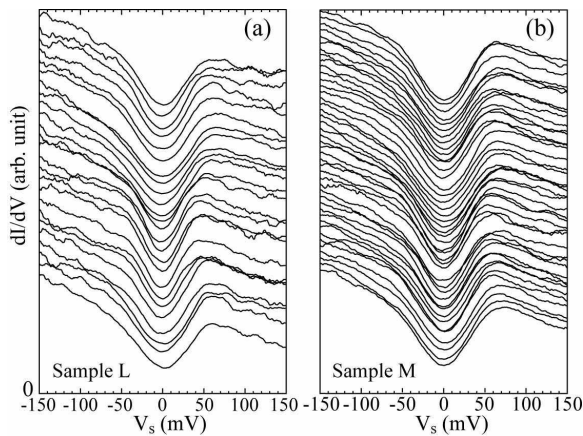


FIG. 3: STS spectra measured along the white lines in the images of Fig. 2. The labels (a) and (b) in Fig. 3 correspond to those in Fig. 2. The spectra are normalized with the value at $V_s = -150$ mV and shifted along the vertical axis for clarity. The zero level in the vertical axis is for the lowest spectrum.

the PG state, respectively. It should be remembered here that samples L and M also exhibit strong and weak CO's (Figs. 2 (d) and (e)) at $T \ll T_c$, respectively. These facts tempt us to suppose that if the $\sim 4a \times 4a$ CO develops markedly in the PG state above T_c , it will continue to exist in the SC state below T_c .

As reported in Ref. 6, in samples exhibiting the strong CO at $T \ll T_c$, the spatial dependence of the energy gap structure is inhomogeneous on the nanometer scale, and vice versa. We will demonstrate in the following paragraphs that such a correlation between the CO and the gap inhomogeneity also holds in the PG state above T_c , which strongly supports the contention that the CO in the SC state will be the same as that in the PG state.

Figures 3 (a) and (b) are tunneling conductance dI/dV - V_s curves, referred to as STS spectra, which were measured along the solid lines in Figs. 2 (a) and (b), STM images of samples L and M, respectively. Similar PG structures are seen in the STS spectra, regardless of the sample and position. The dI/dV value, which tends to increase gradually with the lowering of V_s , is largely reduced in the range around $V_s = 0$, corresponding to E_F ; thus, it exhibits a broad peak around the positive voltage V_s^P , while a broad bend appears around $-V_s^P$ in the negative V_s -region. Here, we define the energy size of PG, Δ_{PG} , from the peak position, V_s^P ; $\Delta_{PG} \equiv eV_s^P$.

Comparing the two sets of STS spectra in Fig. 3, it is found that the Δ_{PG} value changes as a function of position for sample L (Fig. 2 (a)), which exhibits a strong CO, while it is more homogeneous for sample M (Fig. 2 (b)), which exhibits a very weak CO; the average PG values for the two samples are almost the same (~ 60 meV), meaning that they have little difference in p , but the standard deviation (7.0 meV) for sample L is ~ 3 times

larger than that (2.5 meV) for sample M. Such a difference in the spatial inhomogeneity of Δ_{PG} between the two samples can be seen more clearly in 3D illustrations (Figs. 4 (b) and (c)) of the STS spectra (Figs. 3 (a) and (b)), where the vertical axis is for tunneling conductance, and the horizontal axes are for bias voltage and position, respectively.

A 3D illustration of STS spectra measured along a straight line in the former area (Fig. 1 (a)) of sample L, which exhibits an intense CO, is shown in Fig. 4 (a), as well. The average Δ_{PG} value for this area, is ~ 90 meV, suggesting that the p value is smaller than that of the other area (Fig. 2 (a)). Since the $\sim 4a \times 4a$ CO instability tends to be enhanced with the lowering of p , the reduction of p will be one of the factors that cause the intense CO [4, 5]. Furthermore, combining the STM image (Fig. 1 (a)) and the corresponding STS spectra (Fig. 4 (a)), one can see that in the area exhibiting the intense CO, the degree of suppression of spectral weights around $V_s = 0$ (E_F), as well as the Δ_{PG} value, changes drastically as a function of position, that is, the PG structure is much more inhomogeneous. Thus, the energy gap inhomogeneity correlates strongly with the development of $\sim 4a \times 4a$ CO in the PG state, as in the SC state.

To understand such a correlation between the electronic CO and the gap inhomogeneity, we have proposed that the CO is dynamic in itself and, if Bi2212 samples involve strong scattering centers for quasiparticles, leading to the gap inhomogeneity, such as crystallographic imperfections, the scattering centers will function as effective pinning centers for the dynamically fluctuating CO and make it static [5]. On the basis of this pinning picture, the dynamically fluctuating CO would be a candidate for the hidden order of the homogeneous PG state and, the degree of development of the static CO, especially in the samples with similar doping levels, can be explained in terms of the density and/or strength of pinning centers.

According to ARPES experiments on UD Bi2212 [9], the PG starts to develop around temperature T^* , well above T_c , on a part of the Fermi surface (FS) near $(\pi/a, 0)$ and evolves gradually toward the node point of the d -wave gap near $(\pi/a, \pi/a)$ with the lowering of T , but an ungapped region still remains around the node point just above T_c , leading to an arc-shaped FS, which is referred to as the Fermi arc (FA). The FS parts, inside and outside the FA, have been considered to consist of coherent and incoherent electronic states, respectively [10, 11, 12, 13, 14]. In light of these facts, we have argued that even if incoherent quasiparticles outside the FA form pairs in the PG state below $\sim T^*$, they cannot establish long-range phase coherence in collective motion, which will be done by the pairing of coherent quasiparticles on the FA, and the energy gap which opens up on the FA below T_c will function as an effective SC gap in determining T_c [15]. It should be remembered here that the PG, which is formed on the incoherent part of

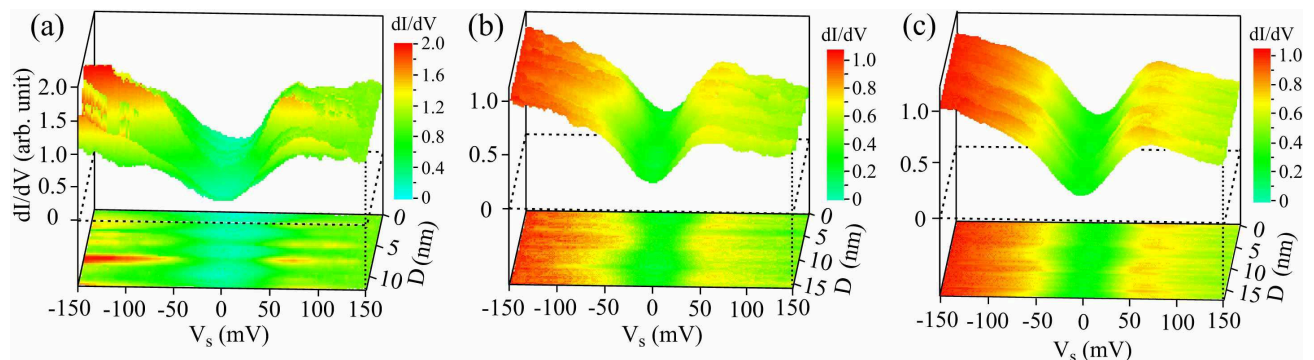


FIG. 4: 3D illustrations of STS spectra, measured along the white lines in Fig. 1 (a), Figs. 2 (a) and (b), respectively. One of the horizontal axes is for the distance (D) from the initial measurement position. Each spectrum in (b) and (c) was normalized with its value at $V_s = -150$ mV, as in Fig. 3, while each spectrum in (a) was normalized with its value at $V_s = 150$ mV because one of the spectra involves a big noise at $V_s = -150$ mV.

the FS, is spatially inhomogeneous in samples exhibiting the strong, pinned $\sim 4a \times 4a$ CO, and vice versa. This fact is naturally understandable, because incoherent electronic states are easily modified by external perturbation, which is due to the randomness associated with pinning potentials for the CO. Furthermore, since the $\sim 4a \times 4a$ CO can be seen in almost the same energy (bias-voltage) range as the PG, incoherent, antinodal quasiparticle or pair states outside the FA will also be responsible for the CO. In fact, it has been found in STM/STS experiments at $T \ll T_c$ that at low energies around E_F , reflecting the quasiparticle states inside the FA, the gap structure is characterized by a spatially-homogeneous d -wave gap and the CO tends to fade out, while at high energies around the gap edge, reflecting the quasiparticle states outside the FA, the gap structure is strongly inhomogeneous and the CO becomes marked [5]. Thus, it is suggested that if the $\sim 4a \times 4a$ CO, which is considered to be dynamic in itself and associated with antinodal quasiparticle or pair states outside the FA, is pinned down and static in the inhomogeneous PG state above T_c , it will remain below T_c , together with the inhomogeneous gap structure in the antinodal region, and coexist with the superconductivity caused by the pairing of coherent quasiparticles on the FA, that is, the so-called “FA superconductivity” [5, 15, 16].

In summary, we performed STM/STS experiments in the PG state above T_c on UD Bi2212, and demonstrated that a strong correlation between the static $\sim 4a \times 4a$ CO and the gap inhomogeneity held in the PG state as in the SC state; the static CO develops markedly in the inhomogeneous PG state, whereas it is very weak in the homogeneous PG state. The static CO can be understood in terms of a pinning picture in which the dynamically fluctuating CO, which seems to be intrinsic in the homogeneous PG and SC states, is pinned down by scattering potentials, leading to gap inhomogeneity. We also sug-

gested that the $\sim 4a \times 4a$ CO is associated with incoherent quasiparticle or pair states on the antinodal FS, which are responsible for the PG, and can coexist with the FA superconductivity below T_c . At the present stage, it is unclear whether a Cooper-pair’s CO or a bosonic CO is realized in high- T_c cuprates. However, the present study will be useful for discussions about the propriety of theoretical models on the $\sim 4a \times 4a$ CO [17, 18, 19, 20, 21].

The authors thank Prof. F. J. Ohkawa for valuable discussions. This work was supported by the 21st century COE program “Topological Science and Technology” and Grants-in-Aid for Scientific Research from the Ministry of Education, Culture, Sports, Science and Technology, Japan.

-
- [1] M. Vershinin *et al.*, *Science* **303**, 1995 (2004).
 - [2] J. E. Hoffman *et al.*, *Science* **297**, 1148 (2002).
 - [3] C. Howald *et al.*, *Phys. Rev. B* **67**, 014533 (2003).
 - [4] N. Momono *et al.*, *J. Phys. Soc. Jpn.* **74**, 2400 (2005).
 - [5] A. Hashimoto *et al.*, *Phys. Rev. B* **74**, 064508 (2006).
 - [6] M. Oda *et al.*, *Physica C* **281**, 135 (1997).
 - [7] M. Oda *et al.*, *Phys. Rev. B* **53**, 2253 (1996).
 - [8] T. Hanaguri *et al.*, *Nature* **430**, 1001 (2004).
 - [9] M. R. Norman *et al.*, *Nature* **392**, 157 (1998).
 - [10] D. Pines, *Physica C* **282-287**, 273 (1997).
 - [11] V. B. Geshkenbein *et al.*, *Phys. Rev. B* **55**, 3173 (1997).
 - [12] N. Furukawa *et al.*, *Phys. Rev. Lett.* **81**, 3195 (1998).
 - [13] X.-G. Wen and P. A. Lee, *Phys. Rev. Lett.* **80**, 2193 (1998).
 - [14] Y. Yanase and K. Yamada, *J. Phys. Soc. Jpn.* **68**, 548 (1999).
 - [15] M. Oda *et al.*, *J. Phys. Soc. Jpn.* **69**, 983 (2000).
 - [16] K. McElroy *et al.*, *Phys. Rev. Lett.* **94**, 197005 (2005).
 - [17] S. A. Kivelson *et al.*, *Nature* **393**, 550 (2001).
 - [18] M. Bosch *et al.*, *Phys. Rev. B* **63**, 092501 (2001).
 - [19] D. Podlosky *et al.*, *Phys. Rev. B* **67**, 094514 (2003).
 - [20] Z. Tesanovic, *Phys. Rev. Lett.* **93**, 217004 (2004).

[21] F. J. Ohkawa, Phys. Rev. B **73**, 092506 (2006).